Chromopolarizabilities of bottomonia from the $\Upsilon(2S, 3S, 4S) \to \Upsilon(1S, 2S)\pi\pi$ transitions

Yun-Hua Chen[1,*] and Feng-Kun Guo[2,3,†]

[1]*School of Mathematics and Physics, University of Science and Technology Beijing, Beijing 100083, China*
[2]*CAS Key Laboratory of Theoretical Physics, Institute of Theoretical Physics,*
Chinese Academy of Sciences, Beijing 100190, China
[3]*School of Physical Sciences, University of Chinese Academy of Sciences, Beijing 100049, China*

The dipion transitions $\Upsilon(2S, 3S, 4S) \to \Upsilon(1S, 2S)\pi\pi$ are systematically studied by considering the mechanisms of the hadronization of soft gluons, exchanging the bottomoniumlike Z_b states, and the bottom-meson loops. The strong pion-pion final-state interaction, especially including the channel coupling to $K\bar{K}$ in the S-wave, is taken into account in a model-independent way using the dispersion theory. Through fitting to the available experimental data, we extract values of the transition chromo-polarizabilities $|\alpha_{\Upsilon(mS)\Upsilon(nS)}|$, which measure the chromoelectric couplings of the bottomonia with soft gluons. It is found that the Z_b exchange has a slight impact on the extracted chromopolarizablity values, and the obtained $|\alpha_{\Upsilon(2S)\Upsilon(1S)}|$ considering the Z_b exchange is (0.29 ± 0.20) GeV^{-3}. Our results could be useful in studying the interactions of bottomonium with light hadrons.

I. INTRODUCTION

The chromopolarizability of a heavy quarkonium state parametrizes the effective interaction of the quarkonium with soft gluons, and it is an important quantity in describing the interactions of quarkonium with hadrons [1–8]. The heavy quarkonium chromopolarizability became interesting recently because of two reasons. First, it is relevant for the interpretation of the structures of multiquark hadrons containing a pair of heavy quark and antiquark. In the hadro-quarkonium picture for hidden-flavor tetraquarks and the baryoquarkonium picture for pentaquarks, the compact heavy quark-antiquark pair is embedded in the light quark matter, and the interaction between these two components takes place via multigluon exchanges. At reasonable values of the chromopolarizabilities of the charmonia, several hadrocharmonium bound states and baryocharmonium bound states are found and identified with certain XYZ states and the P_c^+ pentaquark states [8–12] (a lattice study of the possibility of hadroquarkonium can be found in Ref. [13]). Also, several hidden-bottom bound states are predicted through the study of the spectrum of the

hadrobottomonium and baryobottomonium, and the emergence of these bound states is sensitive to the value of the bottomonium chromopolarizability [14,15]. Secondly, it was suggested that the near-threshold production of heavy quarkonium is sensitive to the trace anomaly contribution to the nucleon mass [16], which may be measured at Jefferson Laboratory and future electron-ion colliders [17] (for a recent discussion, see Ref. [18]). The suggestion is based on the vector-meson dominance model and the assumption that the nucleon interacts with the heavy quarkonium through the exchange of gluons. We notice that, however, the $\Lambda_c^+ D^-$ threhsold is only 116 MeV above the $J/\psi p$ threshold, making the contribution from the $\Lambda_c \bar{D}$ channel to the $J/\psi p$ near-threshold production non-negligible. The $\Lambda_b B$ threshold is more than 500 MeV above the Υp threshold. As a result the Υp near-threshold photoproduction could be a better process for that purpose, and the chromopolarizability for the Υ needs to be understood well first.

The diagonal chromopolarizability α_{QQ}, with Q representing a heavy quarkonium, cannot be extracted directly from the present experimental data. A possible approach to calculate α_{QQ} is based on considering the heavy quarkonia as purely Coulombic systems. This could be a reasonable approximation for the ground state bottomonia, while it is questionable for charmonia and excited bottomonia [15]. On the other hand, the determination of the nondiagonal (transition) chromopolarizability $\alpha_{Q'Q} \equiv \alpha_{Q' \to Q}$ is of importance since it is natural to expect that each of the diagonal amplitudes should be larger than the nondiagonal amplitude; thus the transition chromopolarizability acts a

*yhchen@ustb.edu.cn
†fkguo@itp.ac.cn

reference benchmark for either of the diagonal terms [8,19]. The phenomenological value of the bottomonium transition chromopolarizability $\alpha_{\Upsilon(2S)\Upsilon(1S)}$ has been extracted from the process of $\Upsilon(2S) \to \Upsilon(1S)\pi\pi$, and the result is $|\alpha_{\Upsilon(2S)\Upsilon(1S)}| \approx 0.66$ GeV^{-3} [9,19], where the $\pi\pi$ final-state interaction (FSI) was not considered. Taking account of the $\pi\pi$ S-wave FSI in a chiral unitary approach, it is found that the value of $|\alpha_{\Upsilon(2S)\Upsilon(1S)}|$ may be reduced to about 1/3 of that without the $\pi\pi$ FSI [20]. All these previous studies did not consider the effects of the two bottomoniumlike exotic states $Z_b(10610)$ and $Z_b(10650)$ discovered in channels including $\Upsilon(nS)\pi$ ($n = 1, 2, 3$) by the Belle Collaboration in 2011 [21,22]. In our previous studies which focus on describing the $\pi\pi$ invariant mass spectrum, we found that the $Z_b(10610)^\pm$ and $Z_b(10650)^\pm$ bottomoniumlike states, though being virtual, play a special role in the hadronic transitions $\Upsilon(4S, 3S, 2S) \to \Upsilon(nS)\pi\pi$ [23,24]. Thus the discovery of two Z_b resonances necessitates a reanalysis of the transition chromopolarizabilities in the dipion transitions between the Υ states. In addition, there have been new measurements after our analysis in Refs. [23,24] by the Belle Collaboration with statistics higher than before, and especially they measured the angular distributions of the $\Upsilon(4S) \to \Upsilon(1S, 2S)\pi\pi$ transitions for the first time [25]. These new data help us to perform a comprehensive analysis of the $\Upsilon(4S, 3S, 2S) \to \Upsilon(nS)\pi\pi$ processes.

Since the $\Upsilon(4S)$ meson is above the $B\bar{B}$ threshold and decays predominantly to $B\bar{B}$, the intermediate bottom-meson loops need to be taken into account in the analysis of the $\Upsilon(4S, 3S, 2S) \to \Upsilon(nS)\pi\pi$ processes. The $\pi\pi$ FSI plays an important role in the heavy quarkonium transitions and modifies the value of transition chromopolarizability significantly [20,26], and it is thus necessary to account for its effects properly. In this work we use the dispersion theory in the form of modified Omnès solutions to consider the FSI.[1] The sum of the Z_b-exchange mechanism and the bottom meson loops provide the left-hand-cut contribution to the dispersion integral representation [23,24].

This paper is organized as follows. In Sec. II, we introduce the theoretical framework. In Sec. III, we present the fit results and discuss the phenomenology. Summary and conclusions are given in Sec. IV.

II. THEORETICAL FRAMEWORK

First we define the Mandelstam variables for the decay process $\Upsilon(mS)(p_a) \to \Upsilon(nS)(p_b)\pi(p_c)\pi(p_d)$,

$$s = (p_c + p_d)^2, \quad t = (p_a - p_c)^2, \quad u = (p_a - p_d)^2, \quad (1)$$

where $p_{a,b,c,d}$ are the corresponding four-momenta.

---

[1]The $\pi\pi$ FSI may also be implemented through the generalized distribution amplitude as discussed in Refs. [27,28].

The standard mechanism for these transitions was thought to be the emission of soft gluons from compact bottomonium, followed by their hadronization into two pions. For the bottomonium size being much smaller than the gluon wave length, such a mechanism may be calculated by the nonperturbative quantum chromodynamics (QCD) multipole expansion method, and the amplitude for the dipion transition between S-wave states A and B of heavy quarkonium can be written as [2,29]

$$M_{AB} = 2\sqrt{m_A m_B}\alpha_{AB}\langle\pi^+(p_c)\pi^-(p_d)|\frac{1}{2}\mathbf{E}^a \cdot \mathbf{E}^a|0\rangle$$

$$= \frac{8\pi^2}{b}\sqrt{m_A m_B}\alpha_{AB}(\kappa_1 p_c^0 p_d^0 - \kappa_2 p_c^i p_d^i), \quad (2)$$

where the factor $2\sqrt{m_A m_B}$ appears due to the relativistic normalization of the decay amplitude M_{AB}, α_{AB} is the transition chromopolarizability, $\mathbf{E}^a$ denotes the chromo-electric field, and the second line is from trace anomaly. Here, $b = \frac{11}{3}N_c - \frac{2}{3}N_f$ refers to the first coefficient of the QCD beta function, with $N_c = 3$ and $N_f = 3$ being the numbers of colors and of light flavors, respectively, and κ_1 and κ_2 are not independent as $\kappa_1 = 2 - 9\kappa/2$ and $\kappa_2 = 2 + 3\kappa/2$, where the parameter κ can be determined from fitting to data. The above expression can be reproduced by constructing a chiral effective Lagrangian for the contact $\Upsilon(mS) \to \Upsilon(nS)\pi\pi$ transition. Since the spin-dependent interactions are suppressed for heavy quarks, the heavy quarkonia can be expressed in terms of spin multiplets, and one has $J \equiv \Upsilon \cdot \boldsymbol{\sigma} + \eta_b$, where $\boldsymbol{\sigma}$ contains the Pauli matrices and Υ and η_b annihilate the Υ and η_b states, respectively (see, e.g., Ref. [30]). The effective Lagrangian, at the leading order in the chiral as well as the heavy-quark nonrelativistic expansion, reads [23,24,31]

$$\mathcal{L}_{\Upsilon\Upsilon'\Phi\Phi} = \frac{c_1}{2}\langle J^\dagger J'\rangle\langle u_\mu u^\mu\rangle + \frac{c_2}{2}\langle J^\dagger J'\rangle\langle u_\mu u_\nu\rangle v^\mu v^\nu + \text{H.c.}, \quad (3)$$

where $u_\mu = -\partial_\mu\Phi/F_\pi + \mathcal{O}(\Phi^3)$, with $\Phi = \boldsymbol{\tau} \cdot \boldsymbol{\pi}$ being the pion fields, $\boldsymbol{\tau}$ the Pauli martices, and $F_\pi = 92.1$ MeV the pion decay constant, is the axial current collecting the Goldstone bosons (pions) of the spontaneous breaking of chiral symmetry, and $v^\mu = (1, \mathbf{0})$ is the velocity of the heavy quark. The contact term amplitude obtained by using the chiral Lagrangian in Eq. (3) reads

$$M(s, t, u) = -\frac{4}{F_\pi^2}(c_1 p_c \cdot p_d + c_2 p_c^0 p_d^0). \quad (4)$$

Matching the amplitude in Eq. (2) to that in Eq. (4), we can express the chiral low-energy coupling constants in terms of the chromopolarizability α_{AB} and the parameter κ,

$$c_1 = -\pi^2 \sqrt{m_{\Upsilon'} m_\Upsilon} F_\pi^2 \alpha_{\Upsilon'\Upsilon} \frac{4 + 3\kappa}{b},$$

$$c_2 = 12\pi^2 \sqrt{m_{\Upsilon'} m_\Upsilon} F_\pi^2 \alpha_{\Upsilon'\Upsilon} \frac{\kappa}{b}. \qquad (5)$$

In addition to the multipole contribution $\Upsilon(mS) \to \Upsilon(nS) + \text{gluons} \to \Upsilon(nS)\pi\pi$ which has been parametrized into the chiral contact terms in Eq. (3), we also take into account the mechanisms of the Z_b exchange and the bottom meson loops. In addition, for a complete theoretical treatment of the dipion transitions, as mentioned above, the $\pi\pi$ FSI needs to be taken into account as well. It is considered using the dispersion theory which has been fully described in our previous papers [23,24] (the left-hand cuts from the bottom-meson loops are not considered in Ref. [24]), and we only list the relevant Lagrangians for defining the parameters in the following. The relevant Feynman diagrams for the $\Upsilon(mS) \to \Upsilon(nS)\pi\pi$ processes are displayed in Fig. 1.

The leading order chiral Lagrangian for the $Z_b \Upsilon \pi$ interaction reads [30]

$$\mathcal{L}_{Z_b \Upsilon \pi} = \sum_{j=1,2} \sum_n C_{Z_{bj}\Upsilon(lS)\pi} \Upsilon^i(nS) \langle Z_{bj}^{i\,\dagger} u_\mu \rangle v^\mu + \text{H.c.}, \qquad (6)$$

where Z_{b1} and Z_{b2} are used to refer to the $Z_b(10610)$ and $Z_b(10650)$, respectively. The mass difference between the two Z_b states is much smaller than the difference between their masses and the $\Upsilon(nS)\pi$ thresholds; they have the same quantum numbers and thus the same coupling structure as dictated by Eq. (6). As a result, they can hardly be distinguished from each other in the processes studied here, so we only use one effective Z_b state, the $Z_b(10610)$, to include the Z_b effects as done in Refs. [23,24].

To calculate the box diagrams, we need the effective Lagrangian for the coupling of the bottomonium fields to the bottom and antibottom mesons [32],
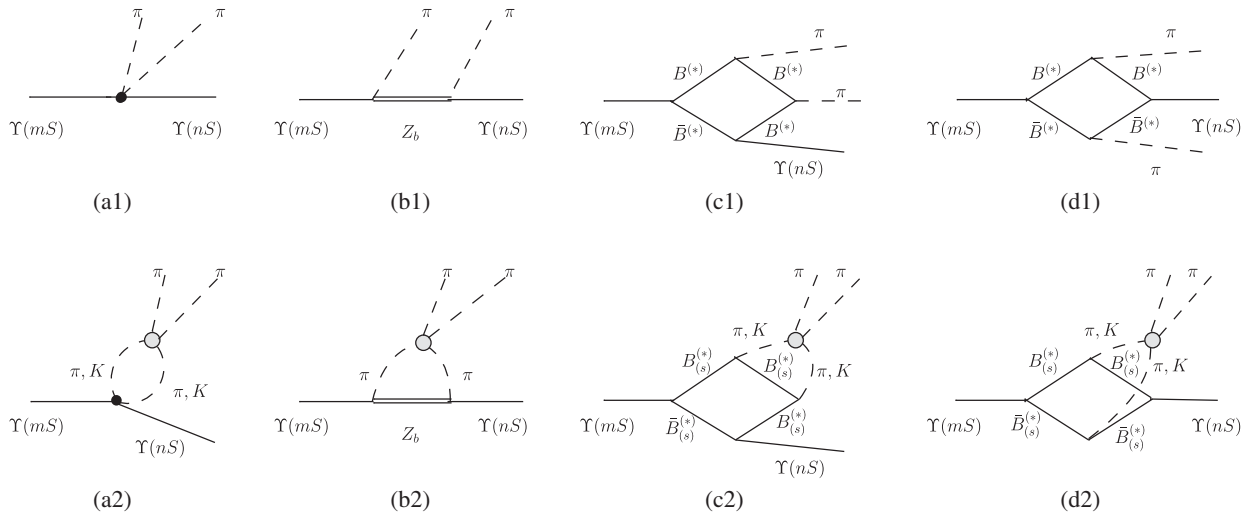
$$\mathcal{L}_{JHH} = \frac{ig_{JHH}}{2} \langle J^\dagger H_a \boldsymbol{\sigma} \cdot \overleftrightarrow{\partial} \bar{H}_a \rangle + \text{H.c.}, \qquad (7)$$

and the coupling of the Goldstone bosons to the bottom and antibottom mesons [33–37],

$$\mathcal{L}_{HH\Phi} = \frac{g_\pi}{2} \langle \bar{H}_a^\dagger \boldsymbol{\sigma} \cdot \mathbf{u}_{ab} \bar{H}_b \rangle - \frac{g_\pi}{2} \langle H_a^\dagger H_b \boldsymbol{\sigma} \cdot \mathbf{u}_{ba} \rangle, \qquad (8)$$

where $H_a = \mathbf{V}_a \cdot \boldsymbol{\sigma} + P_a$ with $\boldsymbol{\sigma}$ being the Pauli matrices and $P_a(V_a) = (B^{(*)-}, \bar{B}^{(*)0}, \bar{B}_s^{(*)0})$ [37]. We use $g_\pi = 0.5$ for the axial coupling from a recent lattice QCD calculation [38].

III. PHENOMENOLOGICAL DISCUSSION

For each $\Upsilon(mS) \to \Upsilon(nS)\pi\pi$ transition, the unknown parameters include the chromopolarizability $\alpha_{\Upsilon(mS)\Upsilon(nS)}$, the parameter $\kappa_{\Upsilon(mS)\Upsilon(nS)}$, the product of couplings for the effective Z_b-exchange $C_{Z_b\Upsilon(mS)\pi} C_{Z_b\Upsilon(nS)\pi}$, and the product of couplings for the box diagrams $g_{JHH(mS)}g_{JHH(nS)}$. The value of $g_{JHH(4S)}$ can be extracted from the measured open-bottom decay widths of the $\Upsilon(4S)$, $g_{JHH(4S)} = 1.43 \, \text{GeV}^{-3/2}$. The unknown couplings $g_{JHH(1S)}$, $g_{JHH(2S)}$, and $g_{JHH(3S)}$ are fixed from simultaneously fitting to the experimental data of the $\pi\pi$ invariant mass distributions and the helicity angular distributions of the $\Upsilon(2S) \to \Upsilon(1S)\pi\pi$, $\Upsilon(3S) \to \Upsilon(1S)\pi\pi$, and $\Upsilon(4S) \to \Upsilon(1S, 2S)\pi\pi$ processes.

The results of the best fit are shown as the solid black (solid magenta) curves for the $\pi^+\pi^-$ ($\pi^0\pi^0$) mode in Fig. 2. The fitted parameters as well as the $\chi^2/(\text{number of events})$ for each $\Upsilon(mS) \to \Upsilon(nS)\pi\pi$ transition are given in Table I. Using the central values of the parameters in the best fit, in Fig. 3 we plot the moduli of the S- and D-wave
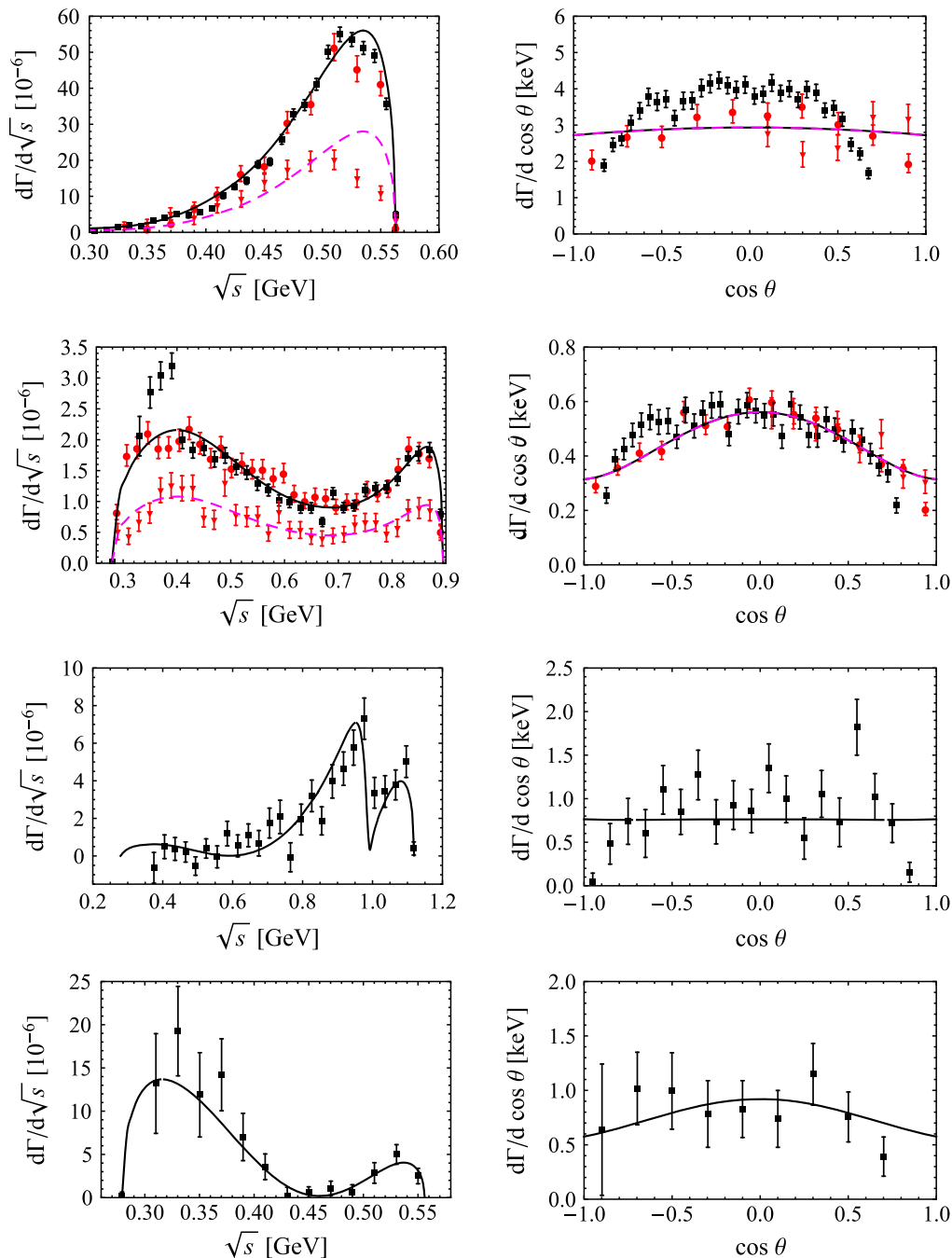

FIG. 1. Feynman diagrams considered for the $\Upsilon(mS) \to \Upsilon(nS)\pi\pi$ processes. The crossed diagrams of (b1), (c1), (b2), and (c2) are not shown explicitly. The gray blob denotes the FSI.

FIG. 2. Fit results for the decays $\Upsilon(2S) \to \Upsilon(1S)\pi\pi$, $\Upsilon(3S) \to \Upsilon(1S)\pi\pi$, $\Upsilon(4S) \to \Upsilon(1S)\pi^+\pi^-$, and $\Upsilon(4S) \to \Upsilon(2S)\pi^+\pi^-$ (from top to bottom). The left panels display the $\pi\pi$ invariant mass spectra, while the right panels show the $\cos\theta$ distributions. The solid squares denote the charged decay mode data from the Belle Collaboration [25]. The solid circles and solid triangles denote the charged and neutral decay mode data, respectively, from the CLEO Collaboration [39]. The solid black and solid magenta lines show the best fit results for charged- and neutral-pion final states.

amplitudes from the chiral contact terms, the effective Z_b exchange, and the box graphs for each $\Upsilon(mS) \to \Upsilon(nS)\pi\pi$ transition.

Several remarks about the fitting results are in order:

(1) For the $\Upsilon(2S) \to \Upsilon(1S)\pi\pi$ process, there are large discrepancies between our theoretical output and the angular distribution data measured by Belle.

As shown in Fig. 3, for the dominant chiral contact terms and the Z_b-exchange term, their D-wave components are about 1 order of magnitude smaller than the corresponding S-wave ones. Thus, a rather flat angular distribution is expected in our scheme, which agrees with the CLEO measurement, but not with the Belle measurement. In addition, one notices that in the
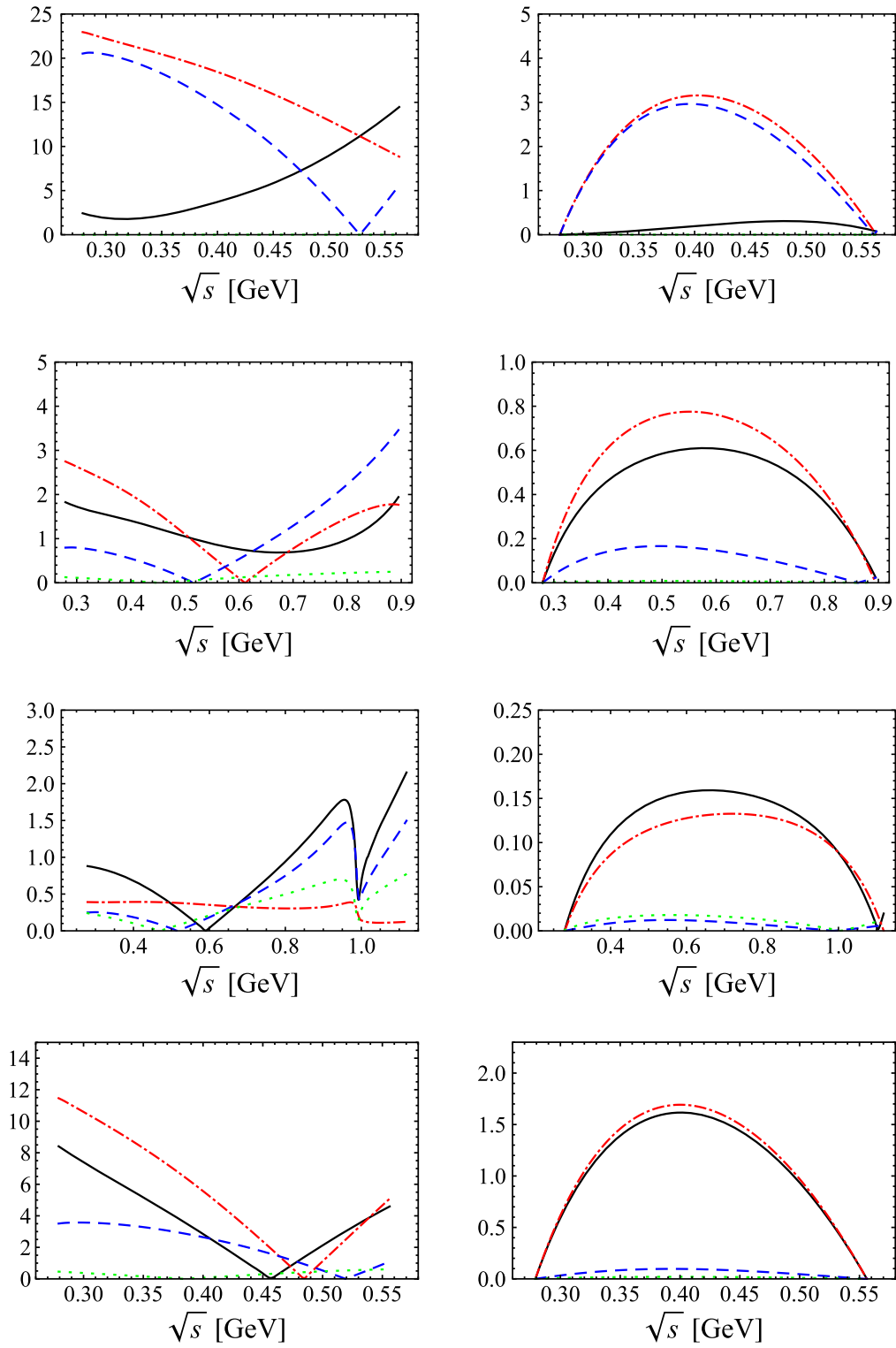
FIG. 3. Moduli of the S- (left) and D-wave (right) amplitudes in the decays $\Upsilon(2S) \to \Upsilon(1S)\pi\pi$, $\Upsilon(3S) \to \Upsilon(1S)\pi\pi$, $\Upsilon(4S) \to \Upsilon(1S)\pi^+\pi^-$, and $\Upsilon(4S) \to \Upsilon(2S)\pi^+\pi^-$ (from top to bottom). The black solid lines represent our best fit results, while the red dot-dashed, blue dashed, and green dotted lines correspond to the contributions from the chiral contact terms, the Z_b, and the box diagrams, respectively.

$\psi' \to J/\psi\pi\pi$ transition, a rather flat angular distribution was observed experimentally [40].

For the transition chromopolarizability, considering only the multipole contribution $\Upsilon(mS) \to$ gluons $+ \Upsilon(nS) \to \Upsilon(nS)\pi\pi$ (i.e., the chiral contact terms), the value without FSI was obtained as $|\alpha_{\Upsilon(2S)\Upsilon(1S)}| \approx 0.66$ GeV^{-3} [9,19], and the value including the $\pi\pi$ FSI in a chiral unitary approach is $|\alpha_{\Upsilon(2S)\Upsilon(1S)}| = 0.24 \pm 0.01$ GeV^{-3} [20]. As shown in Table I, the effects of Z_b exchange and the box diagrams modify the value of the chromopolarizability slightly, and now it is $|\alpha_{\Upsilon(2S)\Upsilon(1S)}| = 0.29 \pm 0.20$ GeV^{-3}, which agrees with the result in Ref. [20] within errors.

For the parameter κ, one observes that the value from our fit $\kappa_{\Upsilon(2S)\Upsilon(1S)} = 1.52 \pm 1.17$, carrying a sizeable uncertainty. Its central value is larger than the result $\kappa_{\Upsilon(2S)\Upsilon(1S)} = 0.342^{+0.015}_{-0.017}$ in Ref. [41] using QCD multipole expansion, which was obtained from fitting to the $\pi\pi$ differential decay width spectrum of $\Upsilon(2S) \to \Upsilon(1S)\pi\pi$ using a chiral effective Lagrangian as in Ref. [42]. There are four differences between our treatment and that in Ref. [41]: (1) we have considered $\pi\pi$ FSI, (2) we have considered the Z_b, (3) we have considered the bottom-meson box diagrams, and (4) we dropped the term proportional to the quark mass matrix in the chiral Lagrangian since the same term introduces a $\Upsilon(2S)\Upsilon(1S)$ mixing by virtual of chiral symmetry and should be eliminated upon diagonalizing the mass matrix for the Υ states as argued in [24]. Among them, (2) and (3) are non-multipole effects, and (1) is mandatory in particular for the $\pi\pi S$ wave since the $f_0(500)$ resonance is located in this energy range. Our earlier analysis in Ref. [24], where the bottom-meson box diagrams were not considered, led to a value of -0.13 ± 0.25 for $\kappa_{\Upsilon(2S)\Upsilon(1S)}$.

One observes the following hierarchy from our fit: $|\alpha_{\Upsilon(4S)\Upsilon(1S)}| \ll |\alpha_{\Upsilon(3S)\Upsilon(1S)}| \ll |\alpha_{\Upsilon(2S)\Upsilon(1S)}| \lesssim |\alpha_{\Upsilon(4S)\Upsilon(2S)}|$, which agrees with the expectation in Ref. [19]. This may be qualitatively understood from the node structure of the $\Upsilon(nS)$ wave functions [43,44]: for the processes with the same final Υ state,

the larger the difference between the principal quantum numbers, the smaller the gluonic matrix elements and thus the magnitude of the transition chromopolarizabilities.

(2) For the $\Upsilon(3S) \to \Upsilon(1S)\pi\pi$ process, one observes that the two-hump structure of the $\pi\pi$ mass spectrum and the angular distribution can be well reproduced. One notices that there is a jump at around 0.35 GeV in the Belle data, which, however, is dubious since there is no threshold or any other singularity in that region. The Belle data points below 0.35 GeV contribute sizeably to the value of χ^2.

(3) For the $\Upsilon(4S) \to \Upsilon(1S)\pi^+\pi^-$ process, the dipion mass spectrum indeed has a dip around 1 GeV in the new Belle data, which has been predicted due to the presence of the $f_0(980)$ [23]. We further notice that now the data points left to the $f_0(980)$ are the highest ones and the line shape there is lifted up mainly by the Z_b-exchange mechanism. This feature can be seen in Fig. 3, where one observes that for the dominant S-wave amplitudes, the Z_b exchange plays a major role in the energy range around 0.95 GeV. Thus, the effective couplings of Z_b to $\Upsilon(4S)\pi$ and $\Upsilon(1S)\pi$ are better constrained compared with our previous study [23]. For the angular distribution, the theoretical prediction is very flat since the D-wave contribution is much smaller than the S-wave one.

(4) For the $\pi\pi$ mass spectrum of the $\Upsilon(4S) \to \Upsilon(2S)\pi^+\pi^-$ process, the new Belle data show a two-peak structure as in the old *BABAR* data [45], while a distinct difference is that in the Belle data the dip approaches 0 inside the physical region. Since the chiral contact amplitude contains a 0 in this energy range, the $\pi\pi$ mass spectrum of the Belle data can be described well even by only including the chiral contact terms with FSI as we have checked. As a result, the value of $|g_{JHH(2S)}|$ turns out to be smaller than that determined in Ref. [23] where the *BABAR* data with larger uncertainties [45] were used. In the *BABAR* data, the dip at around 0.45 GeV is higher, leading to a larger value of $|g_{JHH(2S)}|$.

(5) The branching fractions of the decays of both Z_b states into $\Upsilon(nS)\pi$ ($n \leq 3$) have been reported by

TABLE I. Fit parameters from the best simultaneous fit of the $\Upsilon(mS) \to \Upsilon(nS)\pi\pi(n < m \leq 4)$ processes.

	$\Upsilon(2S) \to \Upsilon(1S)\pi\pi$	$\Upsilon(3S) \to \Upsilon(1S)\pi\pi$	$\Upsilon(4S) \to \Upsilon(1S)\pi^+\pi^-$	$\Upsilon(4S) \to \Upsilon(2S)\pi^+\pi^-$
$|\alpha_{\Upsilon(mS)\Upsilon(nS)}|$[GeV^{-3}]	0.29 ± 0.20	0.06 ± 0.03	$(5.4 \pm 3.5) \times 10^{-4}$	0.43 ± 0.01
$\kappa_{\Upsilon(mS)\Upsilon(nS)}$	1.52 ± 1.17	0.34 ± 0.19	-3.3 ± 2.1	0.53 ± 0.02
$\chi^2/$(number of events)	$794.7/98$	$288.4/151$	$75.3/43$	$14.7/23$
	$|C_{Z_{b1}\Upsilon(1S)\pi}|$	$|C_{Z_{b1}\Upsilon(2S)\pi}|$	$|C_{Z_{b1}\Upsilon(3S)\pi}|$	$|C_{Z_{b1}\Upsilon(4S)\pi}|$
	$(5.7 \pm 0.2) \times 10^{-2}$	1.6 ± 0.1	$(2.1 \pm 0.1) \times 10^{-2}$	$(3.3 \pm 0.1) \times 10^{-3}$
	$|g_{JHH(1S)}|$[GeV$^{-3/2}$]	$|g_{JHH(2S)}|$[GeV$^{-3/2}$]	$|g_{JHH(3S)}|$[GeV$^{-3/2}$]	
	$(4.1 \pm 0.2) \times 10^{-5}$	$(2.7 \pm 0.8) \times 10^{-4}$	1.4 ± 5.1	

Belle in Ref. [46], where the Z_b line shapes were fitted using Breit-Wigner forms. If we naively calculated the partial widths by multiplying these branching fractions by the measured widths of the two Z_b states, we would obtain the $Z_{bi}\Upsilon(nS)\pi$ coupling strengths[2]

$$|C^{\text{naive}}_{Z_{b1}\Upsilon(1S)\pi}| = (3.1 \pm 0.5) \times 10^{-3},$$

$$|C^{\text{naive}}_{Z_{b2}\Upsilon(1S)\pi}| = (1.3 \pm 0.3) \times 10^{-3},$$

$$|C^{\text{naive}}_{Z_{b1}\Upsilon(2S)\pi}| = (2.1 \pm 0.3) \times 10^{-2},$$

$$|C^{\text{naive}}_{Z_{b2}\Upsilon(2S)\pi}| = (0.9 \pm 0.2) \times 10^{-2},$$

$$|C^{\text{naive}}_{Z_{b1}\Upsilon(3S)\pi}| = (5.8 \pm 0.9) \times 10^{-2},$$

$$|C^{\text{naive}}_{Z_{b2}\Upsilon(3S)\pi}| = (3.0 \pm 0.5) \times 10^{-2}, \quad (9)$$

by using

$$|C_Z| = \left\{ \frac{4\pi F_\pi^2 m_{Z_b} \Gamma_{Z_b \to \Upsilon\pi}}{m_\Upsilon |\mathbf{p}_f| (m_\pi^2 + \mathbf{p}_f^2)} \right\}^{\frac{1}{2}}, \quad (10)$$

where $|\mathbf{p}_f| \equiv \lambda^{1/2}(m_{Z_b}^2, m_\Upsilon^2, m_\pi^2)/(2m_{Z_b})$. One observes that our results of the coupling strengths for $|C_{Z_{b1}\Upsilon(1S)\pi}|$ and $|C_{Z_{b1}\Upsilon(2S)\pi}|$ in Table I are about 1 or 2 orders of magnitude larger than those listed above, and the values of $|C_{Z_{b1}\Upsilon(3S)\pi}|$ in Table I and in Eq. (9) are of the same order of magnitude. Notice that as analyzed in our previous work [24], the Breit-Wigner parametrization used Ref. [46] is not the appropriate way for describing the Z_b line shapes; the Z_b states are very close to the $B^{(*)}\bar{B}^*$ thresholds, and thus a Flatté parametrization should be used, which would lead to much larger partial widths into $\Upsilon(nS)\pi$, and thus the relevant coupling strengths. For more details, we refer to Ref. [24]. In addition, since both Z_b states are well above the $\Upsilon(4S)$ mass, and their effects in the dipion transitions can be hardly distinguished from each other [24]; thus we have included only one effective Z_b state in our framework. The so-obtained coupling strengths $|C_{Z_{b1}\Upsilon(lS)\pi}|$ in Table I should be understood as effectively containing effects from both of the $Z_b(10610)$ and $Z_b(10650)$ states. Nevertheless, even taking the above two facts into account, the value of $|C_{Z_{b1}\Upsilon(2S)\pi}|$ in Table I is too large since it would lead to a partial width of the GeV order using Eq. (9).

Notice that the Belle data of the $\Upsilon(2S) \to \Upsilon(1S)\pi\pi$ process played a crucial role in fixing the value of $|C_{Z_{b1}\Upsilon(2S)\pi}|$, and as mentioned in the first two remarks, the present Belle data on the $\Upsilon(2S, 3S) \to \Upsilon(1S)\pi\pi$ transitions have some dubious properties. We expect that the future better data of these processes and a proper extraction of the branching fractions of the $Z_{bi} \to \Upsilon(nS)\pi$ ($n \leq 3$) decays may help to solve this discrepancy.

IV. CONCLUSIONS

We have systemically studied the dipion transitions $\Upsilon(mS) \to \Upsilon(nS)\pi\pi$ with $n < m \leq 4$. In addition to the multipole contribution $\Upsilon(mS) \to \Upsilon(nS) + \text{gluons} \to \Upsilon(nS)\pi\pi$, the Z_b exchange and bottom-meson loops are taken into account. The strong coupled-channel ($\pi\pi$ and $K\bar{K}$) FSI is considered model independently by using the dispersion theory. Through fitting the updated data of the $\pi\pi$ invariant mass spectra and the helicity angular distributions, the values of the transition the chromopolarizabilities $|\alpha_{\Upsilon(mS)\Upsilon(nS)}|$ are determined. In particular, we find that after including the Z_b exchange and bottom-meson loops the value of $|\alpha_{\Upsilon(2S)\Upsilon(1S)}|$ is determined to be (0.29 ± 0.20) GeV^{-3}. It is expected in Refs. [8,19] that the off-diagonal chromopolarizability should be somewhat smaller than the diagonal one. Within uncertainties, the value of $|\alpha_{\Upsilon(2S)\Upsilon(1S)}|$ from our determination is similar to the diagonal chromopolarizability $|\alpha_{\Upsilon(1S)\Upsilon(1S)}|$, calculated to be in the range of $[0.33, 0.47]$ GeV^{-3} in Ref. [15] and $0.50^{+0.42}_{-0.38}$ GeV^{-3} in Ref. [47], and yet the central value is indeed smaller. The results obtained in this work would be valuable to understand the chromopolarizabilities of bottomonia, and will have applications for the studies of light-hadron-bottomonia interactions.

ACKNOWLEDGMENTS

---

[2]In [24], the nonrelativistic normalization factor of $\sqrt{M}$ for heavy mesons has been absorbed into the coupling constants, so the coupling constants therein differ from the corresponding ones in Eq. (9) by a factor of $\sqrt{M_{Z_{bi}} M_{\Upsilon(mS)}}$.

[1] M. B. Voloshin and V. I. Zakharov, Phys. Rev. Lett. **45**, 688 (1980).

[2] V. A. Novikov and M. A. Shifman, Z. Phys. C **8**, 43 (1981).

[3] T. Matsui and H. Satz, Phys. Lett. B **178**, 416 (1986).

[4] S. J. Brodsky and G. A. Miller, Phys. Lett. B **412**, 125 (1997).

[5] A. Hayashigaki, Prog. Theor. Phys. **101**, 923 (1999).

[6] T. A. Lähde and D. O. Riska, Nucl. Phys. **A707**, 425 (2002).

[7] F.-K. Guo, P.-N. Shen, H.-C. Chiang, and R.-G. Ping, Nucl. Phys. **A761**, 269 (2005).

[8] A. Sibirtsev and M. B. Voloshin, Phys. Rev. D **71**, 076005 (2005).

[9] M. B. Voloshin, Prog. Part. Nucl. Phys. **61**, 455 (2008).

[10] S. Dubynskiy and M. B. Voloshin, Phys. Lett. B **666**, 344 (2008).

[11] M. I. Eides, V. Y. Petrov, and M. V. Polyakov, Phys. Rev. D **93**, 054039 (2016); Eur. Phys. J. C **78**, 36 (2018).

[12] K. Tsushima, D. H. Lu, G. Krein, and A. W. Thomas, Phys. Rev. C **83**, 065208 (2011).

[13] M. Alberti, G. S. Bali, S. Collins, F. Knechtli, G. Moir, and W. Söldner, Phys. Rev. D **95**, 074501 (2017).

[14] J. Ferretti, Phys. Lett. B **782**, 702 (2018).

[15] J. Ferretti, E. Santopinto, M. Naeem Anwar, and M. A. Bedolla, Phys. Lett. B **789**, 562 (2019).

[16] D. Kharzeev, Proceedings of the International School of Physics "Enrico Fermi" **130**, 105 (1996).

[17] S. Joosten and Z. E. Meziani, Proc. Sci., QCDEV2017 (**2018**) 017.

[18] Y. Hatta and D. L. Yang, Phys. Rev. D **98**, 074003 (2018).

[19] M. B. Voloshin, Mod. Phys. Lett. A **19**, 665 (2004).

[20] F.-K. Guo, P.-N. Shen, and H.-C. Chiang, Phys. Rev. D **74**, 014011 (2006).

[21] I. Adachi (Belle Collaboration), arXiv:1105.4583.

[22] A. Bondar et al. (Belle Collaboration), Phys. Rev. Lett. **108**, 122001 (2012).

[23] Y.-H. Chen, M. Cleven, J. T. Daub, F.-K. Guo, C. Hanhart, B. Kubis, U.-G. Meißner, and B. S. Zou, Phys. Rev. D **95**, 034022 (2017).

[24] Y.-H. Chen, J. T. Daub, F.-K. Guo, B. Kubis, U.-G. Meißner, and B.-S. Zou, Phys. Rev. D **93**, 034030 (2016).

[25] E. Guido et al. (Belle Collaboration), Phys. Rev. D **96**, 052005 (2017).

[26] Y.-H. Chen, Adv. High Energy Phys. **2019**, 7650678 (2019).

[27] M. Diehl, T. Gousset, B. Pire, and O. Teryaev, Phys. Rev. Lett. **81**, 1782 (1998).

[28] M. Diehl, T. Gousset, and B. Pire, Phys. Rev. D **62**, 073014 (2000).

[29] M. B. Voloshin, Pis'ma Zh. Eksp. Teor. Fiz. **37**, 58 (1983) [JETP Lett. **37**, 69 (1983)].

[30] M. Cleven, F.-K. Guo, C. Hanhart, and U.-G. Meißner, Eur. Phys. J. A **47**, 120 (2011).

[31] T. Mannel and R. Urech, Z. Phys. C **73**, 541 (1997).

[32] F.-K. Guo, C. Hanhart, and U.-G. Meißner, Phys. Rev. Lett. **103**, 082003 (2009); **104**, 109901(E) (2010).

[33] G. Burdman and J. F. Donoghue, Phys. Lett. B **280**, 287 (1992).

[34] M. B. Wise, Phys. Rev. D **45**, R2188 (1992).

[35] T. M. Yan, H. Y. Cheng, C. Y. Cheung, G. L. Lin, Y. C. Lin, and H. L. Yu, Phys. Rev. D **46**, 1148 (1992); **55**, 5851(E) (1997).

[36] R. Casalbuoni, A. Deandrea, N. Di Bartolomeo, R. Gatto, F. Feruglio, and G. Nardulli, Phys. Rep. **281**, 145 (1997).

[37] S. Fleming and T. Mehen, Phys. Rev. D **78**, 094019 (2008).

[38] F. Bernardoni, J. Bulava, M. Donnellan, and R. Sommer (ALPHA Collaboration), Phys. Lett. B **740**, 278 (2015).

[39] D. Cronin-Hennessy et al. (CLEO Collaboration), Phys. Rev. D **76**, 072001 (2007).

[40] M. Ablikim et al. (BES Collaboration), Phys. Lett. B **645**, 19 (2007).

[41] A. Pineda and J. Tarrús Castellà, arXiv:1905.03794.

[42] T. Mannel and R. Urech, Z. Phys. C **73**, 541 (1997).

[43] Y. P. Kuang and T. M. Yan, Phys. Rev. D **24**, 2874 (1981).

[44] T. M. Yan, Phys. Rev. D **22**, 1652 (1980).

[45] B. Aubert et al. (BABAR Collaboration), Phys. Rev. Lett. **96**, 232001 (2006).

[46] A. Garmash et al. (Belle Collaboration), Phys. Rev. Lett. **116**, 212001 (2016).

[47] N. Brambilla, G. Krein, J. Tarrús Castellà, and A. Vairo, Phys. Rev. D **93**, 054002 (2016).